Nuclear magnetic resonance imaging

Experience with the first 100 cases at Tygerberg Hospital

J. W. LOTZ, A. J. LOXTON, B. ALHEIT, J. A. BEYERS, S. WYNCHANK

Summary

Facilities for magnetic resonance imaging (MRI) have been available in South Africa since November 1985. This article summarizes our experience with this new imaging modality, illustrates normal anatomical features and pathological conditions in sagittal, coronal and axial planes, and compares MRI with computed tomography scans of the same regions.

S Afr Med J 1986; **70**: 99-104.

Medical imaging using the principles of nuclear magnetic resonance is now well established. It depends on a physical principle totally different from all other imaging techniques. Hence it is logical that magnetic resonance imaging (MRI) can supply information which is not available by other means. In addition no ionizing radiation is used, and it is non-invasive and believed to be totally safe for patients without electrophysiological support devices or conducting implants.[1]

The first MRI device installed in the southern hemisphere has been in operation at the Medical Research Council in Parowvallei, CP, since November 1985, and it is appropriate to describe results obtained on investigation of the first 100 patients from Tygerberg Hospital.

Material and methods

This study analyses the first 100 magnetic resonance examinations performed on patients from Tygerberg Hospital. Table I illustrates the distribution of investigations according to anatomical region and Table II illustrates the distribution of neuropathology investigated by MRI. Imaging was performed on a 0,5 Tesla superconducting Elscint Gyrex 500 magnetic resonance imager with two-dimensional Fourier transform technique. Data were collected using a 200 x 256 matrix for brain studies and a 256 x 256 matrix for other anatomical regions. Section thickness varied according to the anatomical region and the lesion under consideration, in axial, sagittal and coronal planes.

Apart from basic instructions and reassurance, no patient preparation, sedation or contrast medium was employed.

The spin-echo technique was predominantly employed and at least two echoes were routinely obtained, resulting in images with increased T_2 weighting. Inversion recovery images were employed in sections of the brain where white/grey matter contrast was of importance.[2]

Department of Radiology, Tygerberg Hospital and University of Stellenbosch, Parowvallei, CP

J. W. LOTZ, M.B. CH.B., M.MED. (RAD. D.), F.F. RAD. (D.) (S.A.), F.R.C.R.

A. J. LOXTON, M.B. CH.B., M.MED. (RAD. D.)

B. ALHEIT, M.B. CH.B., M.MED. (RAD. D.)

J. A. BEYERS, M.B. CH.B., M.MED. (RAD.), M.D.

Research Institute for Medical Biophysics of the South African Medical Research Council, Parowvallei, CP

S. WYNCHANK, M.B. CH.B., D.PHIL., F. INST. P.

TABLE I. MRI AT TYGERBERG HOSPITAL, NOVEMBER 1985 — FEBRUARY 1986 (100 CASES)

	No. of cases
Brain	50
Vertebral column and spinal content	14
Head and neck	7
Musculoskeletal	7
Thorax	2
Abdomen	9
Pelvis	11
Total	100

TABLE II. MRI OF THE BRAIN (50 CASES)

		No. of cases
Normal		15
Tumours		12
Benign	4	
Malignant	6	
Metastases	2	
Pituitary fossa		8
Tumours	6	
Empty sella	2	
Haematomas		2
Intracerebral	1	
Subdural	1	
Vascular abnormalities		3
Arteriovenous malformation	1	
Haemangioma	1	
Infarcts	1	
Multiple sclerosis		6
Miscellaneous		4
Brain abscess	1	
Hydrocephalus	1	
Arachnoid cyst	1	
Tuberculous granulomas	1	
		50

Results

Some representative results are presented to demonstrate the imaging characteristics of magnetic resonance.

Normal anatomy

Normal anatomical features of the different regions studied are clearly demonstrated in all anatomical planes. Respiratory and cardiac movement degrades images in the thorax and abdomen, but despite this limitation the images obtained are acceptable. Gating facilities will soon be employed locally and should substantially improve thoracic and upper abdominal imaging.

Fig. 1 shows a sagittal section through the human brain. The medial aspects of the cerebral lobe, cerebellum, brainstem, fornix and thalamus are clearly identified.

Fig. 2 is an enlargement of the brainstem and cerebellum; anatomical detail in this sagittal section is remarkably good. The pituitary gland and pituitary stalk are well demonstrated and clearly delineated.

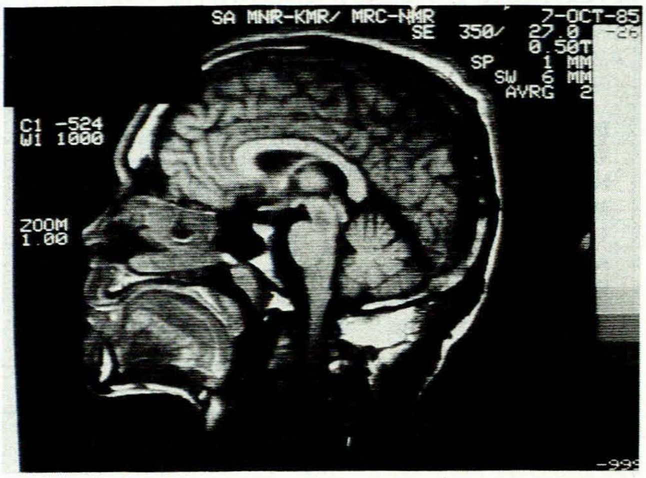

Fig. 1. Median sagittal section of the human brain illustrating normal anatomical features (SE 350/27).

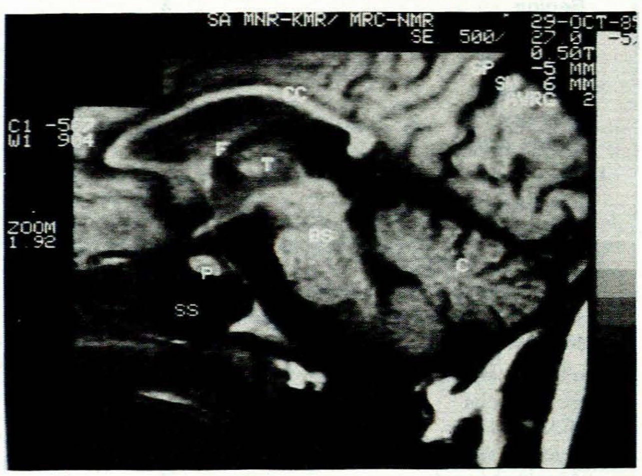

Fig. 2. Sagittal section of the brain, brainstem and spinal cord. The cord is demonstrated to the level of L2 (SE 500/29).

Pathological conditions

Various pathological conditions are presented and where applicable compared with computed tomography (CT) scans of the same anatomical regions. MRI is especially useful for lesions of the brain and spinal cord, but good results were also obtained for abnormalities of the abdomen, pelvis, head and neck, musculoskeletal system and thorax.

Fig. 3a is a sagittal section through the midline of the brain and Fig. 3b an axial section showing mainly the posterior fossa. A large mass lesion with high signal intensity is demonstrated in the pons and brainstem on these relatively T_1-weighted images (SE 500/29). On both sections the centre of the lesion exhibits a low-intensity area and on the axial images there appears to be extension into the right middle cerebral peduncle. These images were interpreted as representing a haemorrhage in the region of the pons and brainstem with extension into the middle cerebellar peduncle

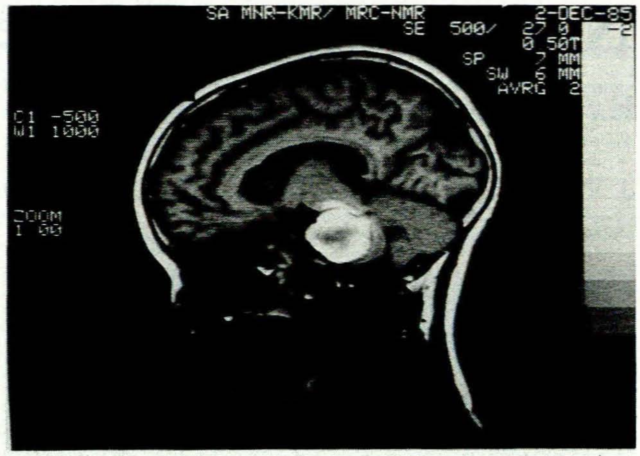

Fig. 3a. Sagittal image of the brain, with a high-intensity brainstem lesion (SE 500/27).

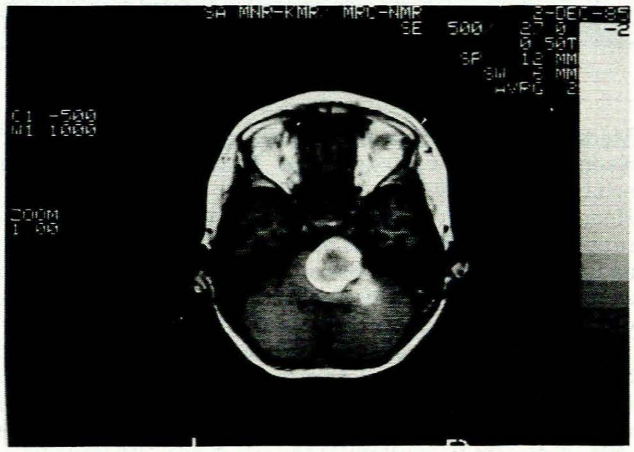

Fig. 3b. Transaxial image of the same lesion obtained on the same day.

on the right. The low-intensity signal in the central region representing an area of liquefaction with a longer T_1 is comparable to the low-intensity signal obtained from fluid surrounding the brain, which appears dark on a T_1-weighted image. Posterior fossa structures are clearly demonstrated and completely free of bone artefact.

On a follow-up scan after approximately 6 weeks the lesion had reduced in size and was surrounded by an area of low-intensity signal representing a halo of oedema. The MRI appearance and clinical progress suggested a haemorrhage in the pons and brainstem area, presumably secondary to a small brainstem haemangioma. The lesion appeared to be undergoing rapid resolution and clinical improvement was in accordance with the MRI observations.

Fig. 4 is a T_2-weighted image (SE 2000/70) of the brain. White matter projects as dark areas owing to a relatively short T_2. Focal pathological areas show as high signal intensity lesions because of a prolongation of T_2 caused by the pathological process. A diagnosis of multiple sclerosis was made on the MRI characteristics and distribution of the lesions.

An MRI in a case of syringomyelia is shown in Fig. 5, with a fluid-filled cavity identified on sagittal images of the dorsal spinal cord. The CSF has a low-intensity signal on these relatively T_1-weighted images, with relatively short TR and TE times in the spin-echo sequence (SE 500/29). There is a fusiform enlargement of the upper dorsal cord and the exact level and extent of the lesion are demonstrated.

Protrusion of the nucleus pulposus at the C3/4 level clearly indents the anterior surface of the spinal cord in a sagittal section through the upper cervical cord (Fig. 6).

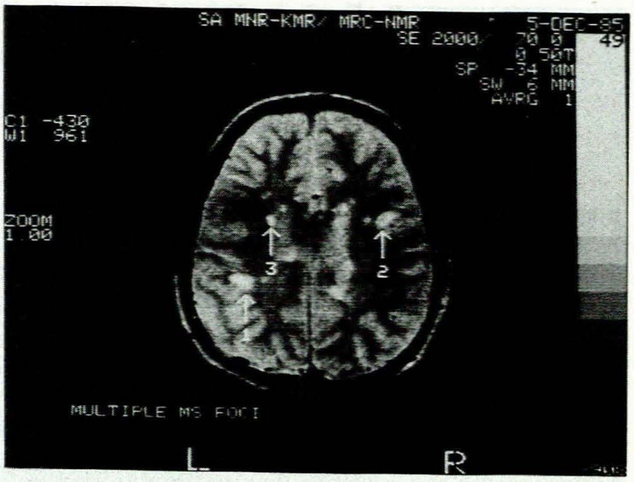

Fig. 4. Multiple sclerosis lesions demonstrated in a T_2-weighted transaxial image (SE 2000/70). The three most prominent lesions are arrowed.

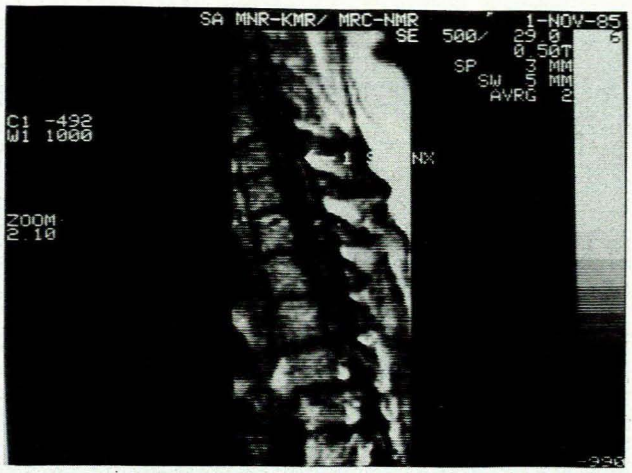

Fig. 5. Syrinx clearly demonstrated on a sagittal image (SE 500/29) of the dorsal spinal cord).

Fig. 6. Sagittal image of the upper cervical cord showing anterior indentation by C3/4 (SE 2000/27).

Figs 7a and 7b are MRIs in a case in which routine chest radiography revealed a large mass lesion in the left paravertebral region. A preliminary diagnosis of a neurogenic tumour was made. CT demonstrated a large paraspinal mass lesion with an intraspinal component causing bone erosion. On the T_2-weighted MRIs the intense signals from the intra- and extra spinal mass are apparent and the configuration and extent of the lesion is much better seen than on CT.

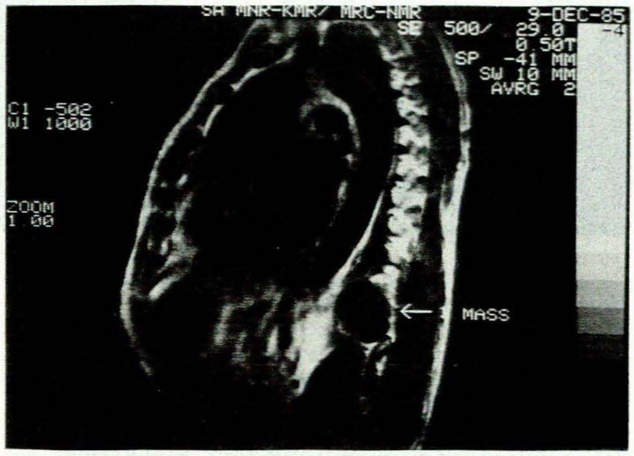

Fig. 7a. Left paravertebral sagittal section showing large paraspinal mass (SE 500/29). The descending aorta is visualized.

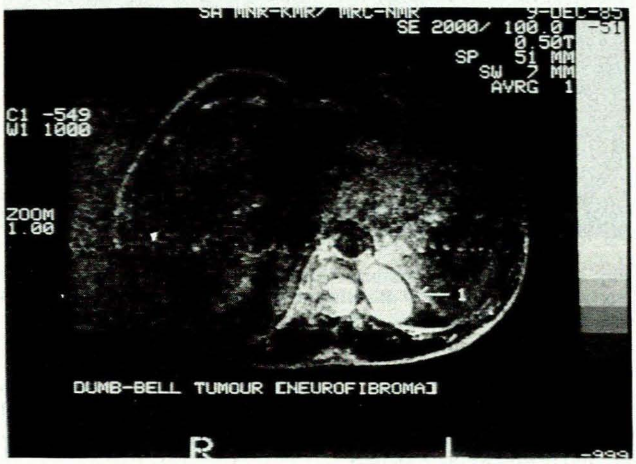

Fig. 7b. T_2-weighted images (SE 2000/100) of the same patient in a transaxial plane highlights dumb-bell-shaped neurofibroma owing to relatively long T_2 value of the lesion.

It is clear from Fig. 7b that with a heavily T_2-weighted image (SE 2000/100) there is deterioration of anatomical detail but marked gain in contrast enhancement due to strong-intensity signals from structures with long T_2 values. The basic principle is that with these long echo times relatively few protons contribute to the image. The only signals that are recovered originate from structures with relatively long T_2 values.[3]

The posterior fossa is notoriously difficult to assess with CT owing to anatomical relief and bone artefact. A case in which it was impossible to assess the posterior fossa with CT owing to an artefact caused by a bismuth iodoform paraffin paste (BIPP) plug in the region of the left mastoid complex is illustrated in Fig. 8a. The MRI, however, clearly demonstrates a large fluid collection in the posterior fossa (Fig. 8b). The image is free of bone artefact, and on this T_2-weighted image no interference was caused by the BIPP plug. A posterior fossa abscess was surgically drained.

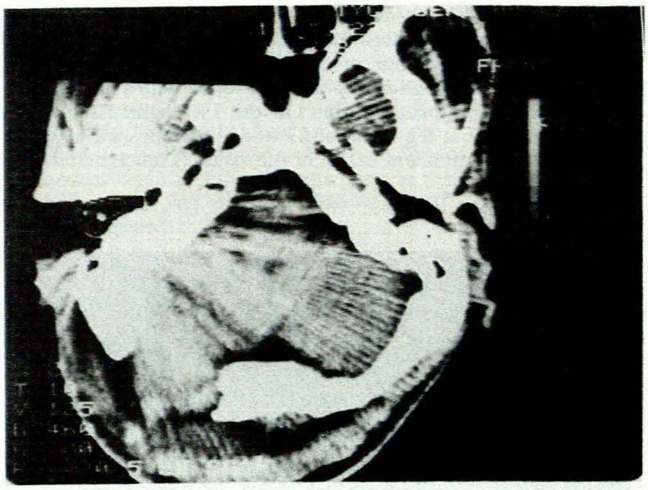

Fig. 8a. CT scan of the posterior fossa. The image is of no diagnostic value owing to an artefact arising from a BIPP plug in the left mastoid region.

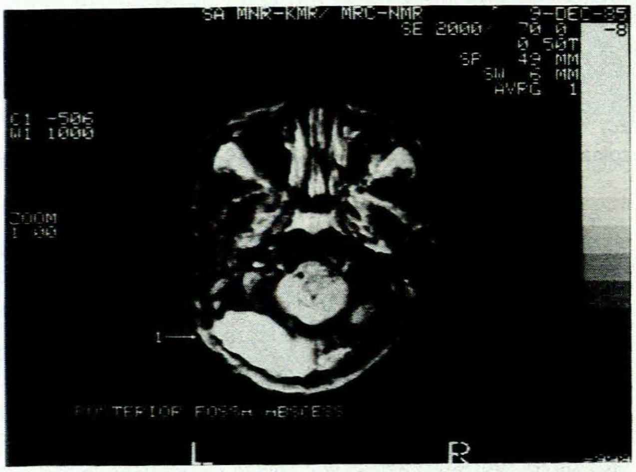

Fig. 8b. MRI of the posterior fossa of the same patient in the transaxial plane clearly showing a large posterior fossa abscess (SE 2000/70).

A large pituitary tumour in sagittal section which extends into the sphenoid sinus is shown in Fig. 9. The exact three-dimensional extent was identified, and the lesion contrasts well with a background of absent bone signals.

Diagnosis of chronic subdural haemorrhage may be difficult on CT, and there are situations in which the isodense subdural haemorrhage cannot be distinguished from the underlying brain parenchyma. Such a case of bilateral subdural haematoma not clearly visualized on CT (Fig. 10a) was investigated with MRI. The image identifies a strong-intensity signal from the blood with a short T_1 value on relatively T_1-weighted images (SE 2000/27).[4] The bilateral subdural haematomas are clearly demonstrated and the lack of bone signals further enhances the remarkable contrast of the image (Fig. 10b).

Sagittal images of the neural cord should be obtained on a relatively T_1-weighted sequence.[5] Adopting this technique, the sagittal section shown in Fig. 11 was obtained in the spin-echo mode with a TR time of 500 ms and a TE time of 29 ms. On these relatively T_1-weighted images the cord has a high-intensity signal, while CSF with a long T_1 appears black. On T_2-weighted images with longer TR and TE times, CSF with a long T_2 gives a stronger signal intensity. This results in a loss of contrast between CSF and the spinal cord. The whole neural canal then appears bright and differentiation is lost. The image now resembles a myelogram examination and extradural impressions are readily recognized.

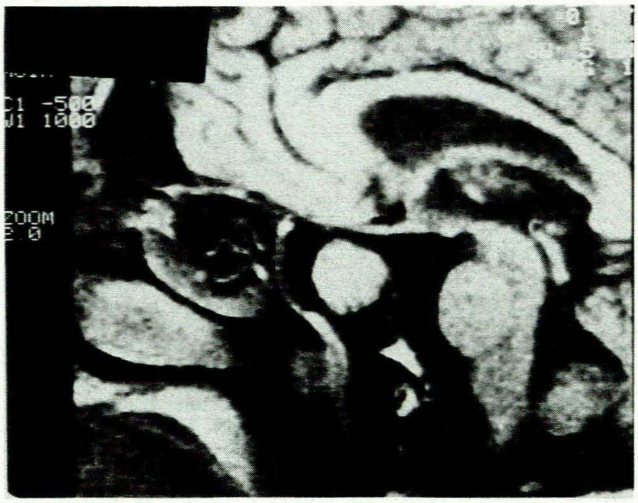

Fig. 9. Pituitary tumour demonstrated in sagittal section (SE 500/27).

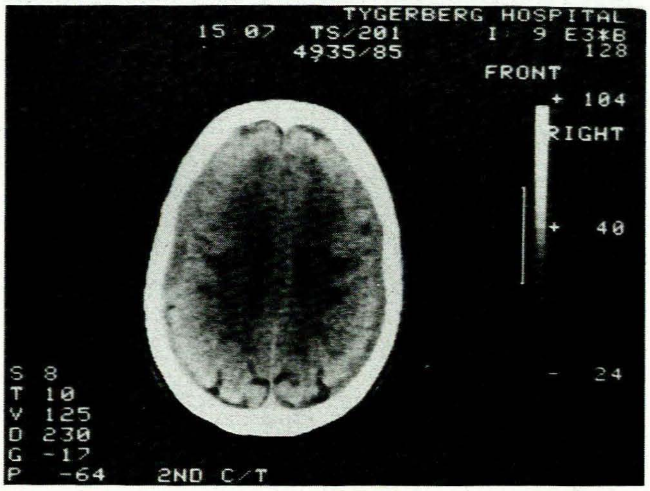

Fig. 10a. Bilateral subdural haematomas are not clearly demonstrated on a CT scan.

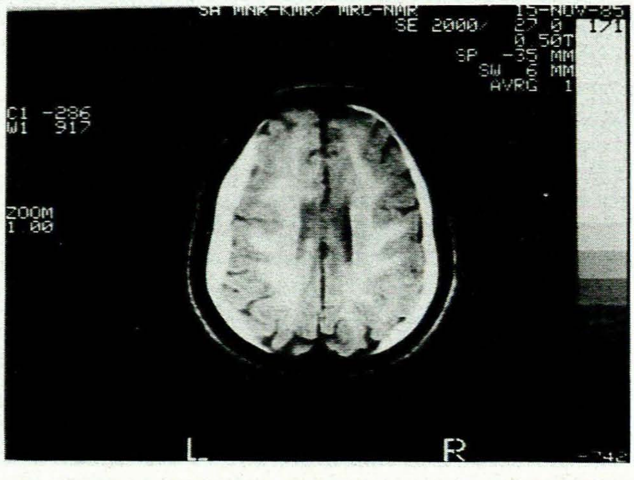

Fig. 10b. Comparable MRI image of the same patient (SE 2000/27) clearly showing bilateral subdural haematomas.

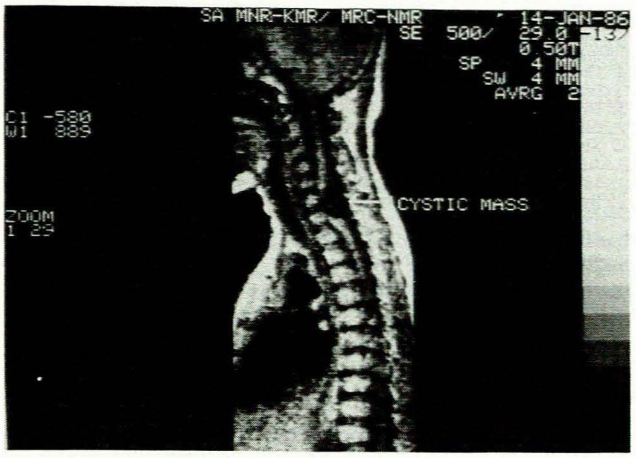

Fig. 11 Low-intensity mass displacing and compressing cervical spinal cord (SE 500/29).

Fig. 11 shows a cystic mass lesion compressing and displacing the cord from behind. The patient had previously been operated on for hydatid disease of the brain and a tentative diagnosis of a hydatid cyst in the cervical spinal cord was made. At operation an intradural hydatid cyst was removed.

Excellent anatomical detail is obtained on sagittal images of the pelvis. The uterine cavity is clearly identified with a relatively strong signal from the endometrium. Pelvic structures are well contrasted against a high-intensity signal from surrounding pelvic fat.

In Fig. 12 the uterus, bladder and rectum are demonstrated in sagittal section. Fibroids are clearly identified on the posterior aspect of the fundus. There is a distinct intensity difference between these benign tumours of smooth muscle and the rest of the uterine muscular wall.

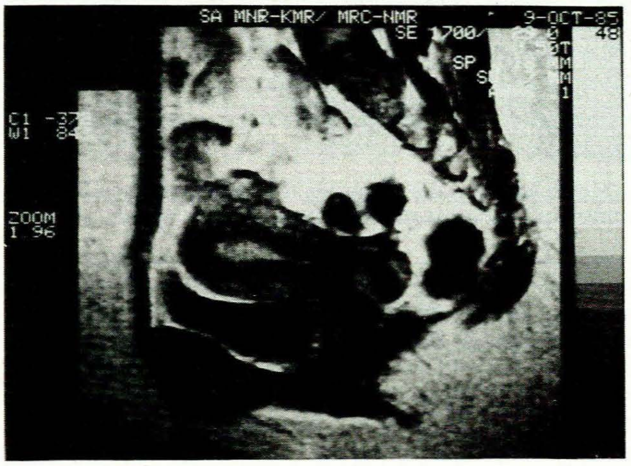

Fig. 12. Anatomical features of the female pelvis clearly demonstrated by MRI (SE 700/29). Fibroids in the posterosuperior fundus can be identified clearly.

Discussion

MRI is a modality which has recently become available in South Africa, and in many respects work on this new technique is still in an experimental phase. Comparative studies, especially with CT, are necessary to assess the relative value of MRI in the diagnostic imaging field.

In our limited experience of 100 cases we found the results of MRI to be in accordance with existing standards in the international literature.

The diagnosis of multiple sclerosis with MRI has recently been documented, and its superiority to CT has been established clearly. MRI was positive in 85% of patients with definite multiple sclerosis, compared with figures for CT ranging from 18% to 47%.[6] MS plaques are clearly defined as areas of increased intensity on T_2-weighted images, while in the inversion recovery sequence, which is T_1-weighted, these lesions which have a long T_1, appear dark owing to low signal intensity.[7] It was possible to identify areas of increased intensity on T_2-weighted images in 6 of 8 patients with clinically suspected multiple sclerosis. The distribution, appearance and long T_2 values of the lesions were consistent with criteria for a positive diagnosis of multiple sclerosis on MRI. In the other 2 cases MRIs were normal. All MRIs were compared with CT scans. In only 2 of the 6 positive cases were there areas of decreased density in cerebral tissues which could not be differentiated from infarcts on CT. Sagittal measurements of the brainstem were performed routinely to assess cord atrophy on the MRIs.

Assessment of the pituitary gland takes on a new dimension with MRI. Sections in three planes are obtainable, and the lack of signal intensity from bone of the sella turcica results in excellent contrast of the pituitary gland against a black background.[8] Demonstration of early micro-adenomas of the pituitary gland on the bases of different T_1 and T_2 values is being investigated.

Excellent images of the dorsal aorta in sagittal section have been obtained, and on coronal images of the abdomen the perinephric and perihepatic spaces are clearly shown. Lesions of the liver were identified on T_2-weighted images as areas of increased intensity due to long T_2 values. Movement artefact, however, detracted from the anatomical detail of the liver, and T_2-weighted images render poor anatomical information owing to low proton signal. It must be emphasized that under these circumstances it is not necessary to obtain an image of good anatomical quality to make a positive diagnosis of metastatic disease.

The pelvic structures are clearly identified and intensity differences exist between endometrium, myometrium and leiomyomas. Diagnosis and staging of pelvic tumours would probably become part of this new technique since organs are clearly contrasted against the high-intensity signal of pelvic fat, and tumour infiltration can therefore be assessed.[9]

At present it is possible to produce images with remarkable anatomical detail. It is also possible to enhance contrast between tissues with different proton content. The major strength of this new technique, however, appears to lie in its ability for soft-tissue differentiation. Theoretically it is possible to assign specific T_1 and T_2 values to different histological tissues for a given magnetic field. By compiling T_1 and T_2 maps of specific anatomical regions it should be possible to obtain an indication of the histological structure of the specific region under consideration. From the current literature there does appear to be overlap of T_1 and T_2 values between normal and pathological tissues. However, using combinations of measured time constants it should theoretically be possible to differentiate benign from malignant tumours, but at present this is not possible routinely and so the degree of overlap limits specificity.

MRI is regarded as a major technological advance in the diagnostic field of medicine, and our observations confirm this. It is envisaged that it will become the prime method of investigation for many pathological conditions and a supportive method of investigation in a very wide area of diagnostic imaging.

We wish to thank the South African Medical Research Council for encouraging utilization of the facility and for permission to publish, the superintendent of Tygerberg Hospital for permission to publish, the Departments of Neurosurgery and Neurology at Tygerberg Hospital for referral of cases, Mrs B. van Dyk, radiographer, for excellent assistance, the Photography Unit of the Bureau for Medical and Dental Education of the University of Stellenbosch for the preparation of the illustrations, and Mrs I. H. Snyders for her help in the preparation of the manuscript.

REFERENCES

1. Wynchank S, Van Heerden PDR. Medical applications of nuclear magnetic resonance. *S Afr Med J* 1985; **67:** 43-48.
2. Smith MA. The technology of magnetic resonance imaging. *Clin Rad* 1985; **36:** 553-559.
3. Smith AS, Weinstein MA, Modu MT *et al.* Magnetic resonance with marked T2-weighted images: improved demonstration of brain lesions, tumor and edema. *AJR* 1985; **145:** 949-955.
4. Gonomi JM, Grossman RI, Goldberg HI *et al.* Intracranial hematomas: imaging by Highfield MR. *Radiology* 1985; **157:** 87-93.
5. How JS, Benson JE, Yoom YS. Magnetic resonance imaging in the spinal column and craniovertebral junction. *Rad Clin North Am* 1984; **22:** 805-827.
6. Sheldon JJ, Siddhorthan R, Tobias J *et al.* MR imaging of multiple sclerosis: comparison with clinical and CT examinations in 74 patients. *AJR* 1985; **145:** 957-964.
7. Bydder GM. Magnetic resonance imaging of the brain. *Rad Clin North Am* 1984; **22:** 779-793.
8. Bilaniuk LT, Zimmerman RA, Wehrli FW *et al.* Magnetic resonance imaging of pituitary lesions using 1,0 to 1,5T field strength. *Radiology* 1984; **153:** 415-418.
9. Fisher MR, Hricak H, Tanagho E. Urinary bladder MR imaging. *Radiology* 1985; **157:** 471-477.

Berekende subtraksie-angiografie

P. A. FOURIE

Summary

Between 10 February 1983 and 9 November 1984 482 patients were investigated by digital subtraction angiography, mainly for carotid arterial disease and problems associated with transplanted kidneys. The use of abdominal compression and antispasmodics are essential to minimize bowel artefacts for intra-abdominal arterial examinations. The apparatus is advantageous for interventional radiologists. Images are immediately seen, can be stored on analogue tape, digitalized and obtained with smaller volumes of contrast medium and without arterial catheterization. Movement artefacts, however, can cause problems.

S Afr Med J 1986; **70:** 104-107.

Gedurende die tydperk 10 Februarie 1983 tot 9 November 1984 (21 maande) is 482 pasiënte met behulp van die berekende subtraksie-angiogramapparaat ondersoek (Tabel I).

Die apparaat is die Gigantos Optimatic 1250R Angiotron met 'n outomatiese driefase-, 12 puls-generator wat 'n konstante 100 kW lewer by 80 - 150 kV en mA wat wissel van 1 250 tot 670 afhangende van die kV, wat òf per hand òf outomaties gereguleer kan word. Die anodefokuspunt is 1 mm^2 en die buis het 'n inherente filtrering van 0,7 mm Al. Die buisomhulsel het 'n 2,5 mm Al-filtrering. Die 278 mm-beeldversterker het 'n resolusie van 4,4 - 5,3 lyne/mm. Filmfokusafstand van 950 - 1 350 mm en televisiematriks van 512 x 512 word gebruik.

Die tegniek van versyfering (digitalisasie) vanaf die analoogsein is reeds deur vorige outeurs beskryf.[1-3]

Departement Radiodiagnostiek, Universiteit van Pretoria en H. F. Verwoerd-hospitaal, Pretoria
P. A. FOURIE, M.MED. (RAD.D.)

Bestraling werk uit op $\pm$ 500 μrad/s tydens opnames.[4]

Soos in Tabel I gesien kan word, is 370 gevalle by wyse van intraveneuse kontrastoediening ondersoek. Hierdie hoë getal intraveneuse kontrastoedienings is te wyte aan die feit dat 111 pasiënte met oorgeplante niere ondersoek is en die intraveneuse roete by al die gevalle gebruik is. Honderd-en-vier gevalle waar nekvate ondersoek is, is ook by wyse van die intraveneuse kontrastoedieningsmetode ondersoek omdat die meeste van hierdie pasiënte as buitepasiënte hanteer is.

Hier volg 'n kort opsomming van bevindings en tegnieke wat gebruik is by die ondersoek van verskillende organe in die liggaam.

Harte

Met behulp van die Angiotron (Siemens) kon geen heksein-studies gedoen word nie, wat wel van groot waarde sou wees

TABEL I. AANTAL GEVALLE EN ROETES VAN KONTRASTOEDIENING

	Arterieel	Veneus	Totaal
Hart		**4**	**4**
Aortaboog	**6**	**49**	**55**
Abdominale aorta		**23**	**23**
Nekvate	**37**	**104**	**141**
A. mammaria interna	**4**		**4**
Renale arteries	**14**	**49**	**63**
Oorgeplante niere		**111**	**111**
Femorale arterie	**14**	**5**	**19**
Intrakraniale arteries	**30**		**30**
Voorarm	**3**	**2**	**5**
Onderbeen		**2**	**2**
Paratiroïede		**11**	**11**
Angioplastiek	**4**		**4**
VCI en VCS		**2+6**	**8**
Pulmonale arteries		**42**	**42**
	112	**370**	**482**

VCI = vena cava inferior. VCS = vena cava superior.